Cardiovascular Research (2016) **111**, 34–43
doi:10.1093/cvr/cvw069

Acute heart failure with cardiomyocyte atrophy induced in adult mice by ablation of cardiac myosin light chain kinase

Michael T. Massengill[1†], Hassan M. Ashraf[1†], Rajib R. Chowdhury[1], Stephen M. Chrzanowski[1], Jeena Kar[1], Sonisha A. Warren[1], Glenn A. Walter[1], Huadong Zeng[2], Byung-Ho Kang[3], Robert H. Anderson[4], Richard L. Moss[5], and Hideko Kasahara[1*]

[1]Department of Physiology and Functional Genomics, University of Florida College of Medicine, 1600 SW Archer Rd, M543, Gainesville, FL 32610-0274, USA; [2]Advanced Magnetic Resonance Imaging and Spectroscopy Facility, University of Florida, Gainesville, FL, USA; [3]Electron Microscopy and Bio-imaging Laboratory, University of Florida, Gainesville, FL, USA; [4]Institute of Genetic Medicine, Newcastle University, Newcastle, UK; and [5]Department of Cell and Regenerative Biology, University of Wisconsin School of Medicine and Public Health, Madison, WI 53706, USA

Received 31 December 2015; revised 1 March 2016; accepted 17 March 2016; online publish-ahead-of-print 29 March 2016

Time for primary review: 34 days

Aims Under pressure overload, initial adaptive hypertrophy of the heart is followed by cardiomyocyte elongation, reduced contractile force, and failure. The mechanisms governing the transition to failure are not fully understood. Pressure overload reduced cardiac myosin light chain kinase (cMLCK) by ~80% within 1 week and persists. Knockdown of cMLCK in cardiomyocytes resulted in reduced cardiac contractility and sarcomere disorganization. Thus, we hypothesized that acute reduction of cMLCK may be causative for reduced contractility and cardiomyocyte remodelling during the transition from compensated to decompensated cardiac hypertrophy.

Methods and results To mimic acute cMLCK reduction in adult hearts, the floxed-*Mylk3* gene that encodes cMLCK was inducibly ablated in *Mylk3*$^{flox/flox}$/*merCremer* mice (*Mylk3-KO*), and compared with two control mice (*Mylk3*$^{flox/flox}$ and *Mylk3*$^{+/+}$/*merCremer*) following tamoxifen injection (50 mg/kg/day, 2 consecutive days). In *Mylk3-KO* mice, reduction of cMLCK protein was evident by 4 days, with a decline to below the level of detection by 6 days. By 7 days, these mice exhibited heart failure, with reduction of fractional shortening compared with those in two control groups (19.8 vs. 28.0% and 27.7%). Severely convoluted cardiomyocytes with sarcomeric disorganization, wavy fibres, and cell death were demonstrated in *Mylk3-KO* mice. The cardiomyocytes were also unable to thicken adaptively to pressure overload.

Conclusion Our results, using a new mouse model mimicking an acute reduction of cMLCK, suggest that cMLCK plays a pivotal role in the transition from compensated to decompensated hypertrophy via sarcomeric disorganization.

Keywords Heart failure • Inducible knockout • Kinase

1. Introduction

In the clinical setting, patients with heart failure suffer extremely high rates of mortality, with up to half dying within 4 years of diagnosis, a progression greater than that for cancer.[1] Despite the development of new and more effective therapies, heart failure remains the leading cause of cardiac death.[2] Under sustained pressure overload, hearts initially exhibit adaptive cardiomyocyte hypertrophy, followed by transitions to failure characterized by maladaptive elongation of cardiomyocytes, and persistent reductions in contractile force. This progression in remodelling is thought to involve an initial adaptive addition of sarcomeres in parallel, producing thickening, and a subsequent addition of sarcomere in series, leading to elongation.[3–6] It is not known, however, whether the addition of sarcomeres occurs in adults in the context of the semi-crystalline architecture of mature cardiomyocytes and the continued production of myocardial force.[3–6]

* Corresponding author. Tel: +1 352 846 1503; fax: +1 352 846 0270, E-mail: hkasahar@ufl.edu

† The first two authors contributed equally to the study.

Studies in the past several decades have shown that the phosphorylation of cardiac myosin light chain 2v (MLC2v) potentiates the rate and force of contraction in the heart.[7–13] The predominant kinase for MLC2v, cardiac *m*yosin *l*ight chain *k*inase (cMLCK), encoded by the *Mylk3* gene, was identified several years ago,[14,15] and confirmed as the predominant MLC2 kinase *in vivo*.[16,17] In cultured cardiomyocytes, overexpression of cMLCK facilitates sarcomeric organization, while its knockdown results in sarcomeric disorganization.[15] A reduction in cMLCK protein was demonstrated as early as 1 week after induction of pressure overload by murine aortic banding or *t*ransverse *a*ortic constriction (TAC), which was shown to coincide with the functional transition from compensated to decompensated hypertrophy within 1–2 weeks of the banding.[17] Unexpectedly, germline cMLCK-deficient ($Mylk3^{-/-}$) mice exhibited compensated cardiac hypertrophy and only moderate heart failure. The mice, however, progressed to severe heart failure under pressure overload.[17]

In the current study, in order to mimic the acute reduction of cMLCK in heart failure, and to understand its effect during transition to heart failure, we have generated tamoxifen-inducible adult *Mylk3* knockout mice. As in the mice that transitioned rapidly to heart failure subsequent to banding-induced pressure overload, we found that our adult *Mylk3* knockout mice also suffered a rapid onset of heart failure.

2. Methods

2.1 Generation of mouse models

A conditional null allele of *Mylk3* was generated as described previously.[17] Germline transmitted mice were crossed with *ACTB-Cre* transgenic mice (Jackson Laboratory, Bar Harbor, ME, USA) to eliminate the *floxed-neomycin-resistant* gene. Mice heterozygous for a *floxed-Mylk3* allele were bred to those expressing the *EIIa-Cre* transgene (Jackson Laboratory, Bar Harbor, ME, USA), resulting in a germline $Mylk3^{flox/+}$ allele. These mice were bred to *αMHCmerCremer* mice,[18] followed by cross-breeding to generate $Mylk3^{+/+}$ and $Mylk3^{flox/flox}$ with or without the *αMHCmerCremer* transgene on a mixed genetic background, mainly C57BL/6. The mice were used at 10–12 weeks of age, with only female mice being subjected to physiological analyses in order to eliminate gender differences in cardiac function. Mice were sacrificed under isoflurane deep anaesthesia or CO_2 inhalation. The TAC operation was performed under sodium pentobarbital anaesthesia (40–60 mg/kg, i.p.), as described previously.[17,19] All animal procedures were performed to conform the NIH guidelines (Guide for the Care and Use of Laboratory Animals) and approved by the University of Florida Institutional Animal Care and Use Committee.

2.2 MRI, echocardiography, and left ventricular pressure–volume measurement

Mice were anaesthetized with 1.5–2% isoflurane supplied either through a nose cone for MRI and echocardiography, or through tracheal intubation for left ventricular pressure–volume (LVPV) measurement. MRI and echocardiography of the hearts were performed as described previously,[17] except for using CINE and HARP software analyses (Diagnosoft, Durham, NC, USA). LVPV measurements using a Millar catheter were performed using standard methods[20] and analysed by PVAN™ as previously described,[19] followed by the conversion of relative volume units to units of volume using the cuvette calibration.

2.3 Measurements of cardiomyocyte size, simultaneous measurements of cell shortening, and intracellular free calcium

Isolated adult cardiomyocytes attached to glass coverslips were imaged under a microscope and digitized for measurements of cell surface area. Rod-shaped cardiomyocytes with clear cross-striations, staircase ends, and surface membranes free from blebs were used for simultaneous measurements of cell shortening and intracellular free calcium (IonOptics, Westwood, MA, USA), as described previously.[17,19,21]

2.4 Western blotting, immunostaining, and histological analyses

Heart tissue was homogenized in acetone containing 10% trichloroacetic acid and 10 mM DTT to fix the phosphorylation status of proteins, centrifuged after 1 h incubation at −20°C, and washed three times with acetone as described previously.[19]

The following antibodies were used: GAPDH (MAB374, EMD Millipore, Billerica, MA, USA), MLC2 (F109.3E1, ALX-BC-1150-S-L005, Enzo Life Science, Farmingdale, NY 11735 USA), phospho-MLC2v (gift from Dr N. Epstein, NIH),[8] cMLCK,[15] troponin T (T6277, Sigma, St. Louis, MO, USA), SERCA2 (SantaCruiz, sc-8095, Dallas, TX, USA), and Ser^{16}-phosphorylated- and total phospholamban (EMD Millipore, Billerica, MA, USA, 07-052, 05-205).

The extent of fibrosis was measured using Picro Sirius red-stained tissue sections. Briefly, the tissue sections were heated at 60°C for 45 min before deparaffinization and stained in 0.1% direct red 80 and 0.1% fast green FCF in 1.2% picric acid for 60 min. Tissue sections were scanned with an Aperio Scanscope CS and analysed by an ImageScope (Leica, Buffalo Grove, IL, USA).

For transmission EM (TEM), hearts were perfused with Tyrode buffer with 20 mM KCl without Ca^{2+} for 5 min, then with the cacodylate buffer with 2% PFA and 2% glutaraldehyde for 5 min. Perfusion-fixed hearts were immersion-fixed in the cacodylate buffer with 2% PFA and 2% glutaraldehyde at 4°C overnight, post-fixed with 1% OsO_4, stained *en bloc* 2% uranyl acetates, embedded in Apon, sectioned, and stained with 4% uranyl acetate/Reynold's lead citrate. Thin sections were examined using a Hitachi H-7000 TEM microscope.

2.5 Real-time RT-PCR

Real-time RT-PCR was performed using inventoried Taqman Gene Expression Assays (TheromoFisher, Waltham, MA, USA): atrial natriuretic factor (ANF) Mm01255748, brain natriuretic peptide (BNP) Mm00435304, skeletal actin Mm0080218, cardiac actin Mm01333821, sarcoendoplasmic reticulum Ca^{2+}-ATPase 2a (SERCA2a) Mm00437634, phospholamban Mm0043318, cardiac ryanodine receptor 2 Mm465877, smooth muscle MLCK Mm00653039, skeletal MLCK Mm01251292, and DAPK3/ZIPK Mm1172884 followed by normalization to β-actin expression (no. 4352933E). Replicated experiments were averaged.

2.6 Statistical analyses

Data presented are expressed as mean values ± SEM. The data, including more than two levels of a repeated-measures factor, were analysed for normal distribution by Levene's test for equality of variances (SPSS ver. 23). Results were compared using Student's *t*-test, ANOVA with or without repeated-measures analyses, nested ANOVA, and Fisher's *post hoc* test. A value of $P < 0.05$ was considered significant (see Supplementary material online, *Table S1* for additional information).

3. Results

3.1 Acute heart enlargement in adult-onset inducible *Mylk3-KO* mice

To mimic the effects of cMLCK reduction observed following TAC,[17] we generated acute *Mylk3-KO* in adult mice using the tamoxifen-inducible Cre recombinase system (*Figure 1A*). Deletion of the floxed exon 5 resulted in elimination of the first coding exon of the catalytic domain and a frameshift of the subsequent downstream exons. In addition,

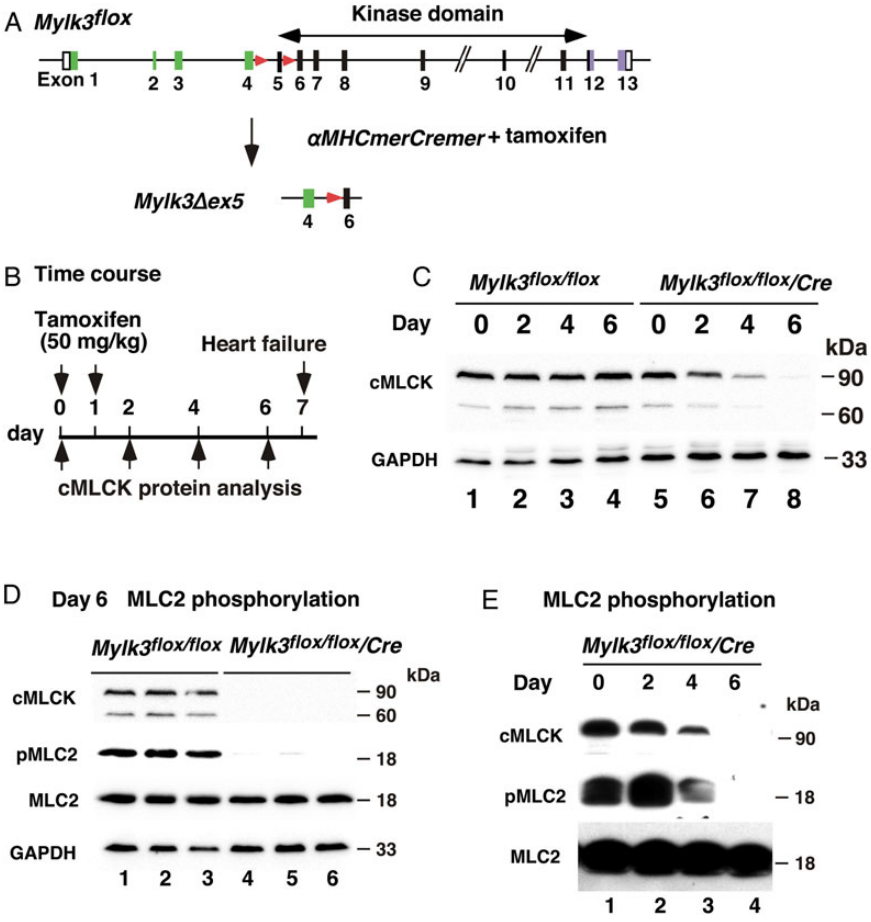

Figure 1 Experimental design of adult-onset inducible *Mylk3-KO* mice leading to acute heart failure. (*A*) Strategy for cardiac tamoxifen-inducible *Mylk3-KO*. (*B*) Timeline of experiments. (*C*) Western blotting demonstrates cMLCK protein expression prior to and 2, 4, and 6 days after tamoxifen injection in *Mylk3*$^{flox/flox}$ with or without the *αMHCmerCremer* transgene. (*D*) MLC2 phosphorylation 6 days after tamoxifen injection in *Mylk3*$^{flox/flox}$ with or without the *αMHCmerCremer* transgene ($n = 3$ each). (*E*) MLC2 phosphorylation prior to and 2, 4, and 6 days after tamoxifen injection in the *Mylk3*$^{flox/flo}$/*αMHCmerCremer* transgene.

deletion of exon 5 resulted in reduction of cMLCK mRNA,[17] attributable to a nonsense-mediated mRNA decay,[22] with targeted cMLCK mRNA containing a premature termination codon.

In this study, the effect of tamoxifen-inducible deletion of the *Mylk3* gene in *Mylk3*$^{flox/flox}$/*αMHCmerCremer* mice, hereafter *Mylk3-KO*, was examined and compared with two control mice (*Mylk3*$^{flox/flox}$ and *Mylk3*$^{+/+}$/*merCremer*) following tamoxifen injection (50 mg/kg/day, 2 consecutive days). This dose of tamoxifen was substantially below the previously reported level of toxicity (i.e. 80 mg/kg/day × 5 days).[23] Day 0 is taken as the day of the first injection (*Figure 1B*).

Expression of cMLCK protein was reduced by Day 4 and was below the level of detection on Day 6 in *Mylk3-KO* following tamoxifen injection (*Figure 1C*). On Day 6, the phosphorylation of the known cMLCK substrate, MLC2v, was markedly reduced in the *Mylk3-KO* hearts (*Figure 1D*). The time course in the reduction in cMLCK protein and MLC2 phosphorylation is shown in *Figure 1E*.

On Day 7, hearts were enlarged in *Mylk3-KO* mice (*Figure 2A*). In particular, when the heart was fixed at end-diastole by retrograde perfusion, the ventricles were noted to be markedly distended, with thinner walls in the hearts from *Mylk3-KO* mice on Days 7 and 14 compared with their controls (*Figure 2B*). The heart weight/body weight (HW/BW) ratio was increased in *Mylk3-KO* compared with control *Mylk3*$^{flox/flox}$ mice (*Figure 2C*). In contrast, *Mylk3*$^{+/+}$/*merCremer* control mice did not show any increase in the HW/BW ratio on Day 14 following tamoxifen injection (*Figure 2D* and *Figure 3B* and see Supplementary material online, *Figure S1*). Increased expression of fetal genes, including ANF, BNP, and skeletal actin, is often observed in failing hearts and was demonstrated in the hearts from *Mylk3-KO* mice on Day 7 (*Figure 2E*).

3.2 Contractile dysfunction in *Mylk3-KO* mice on Day 7

Detailed cardiac function *in vivo* was analysed on Day 7 using MRI, echocardiography, and the left ventricular pressure volume (LVPV) relationship. Representative images obtained using MRI showed increased size of the left and right ventricular cavities at end-diastole in *Mylk3-KO* mice compared with their age- and sex-matched controls (*Mylk3*$^{flox/flox}$ with tamoxifen injection; *Figure 3A*). The hearts from *Mylk3-KO* mice demonstrated statistically increased volumes of the left ventricular cavity both at end-systole and at end-diastole. Decreases in ejection fraction, wall thickness at end-diastole, per cent changes in wall thickness in

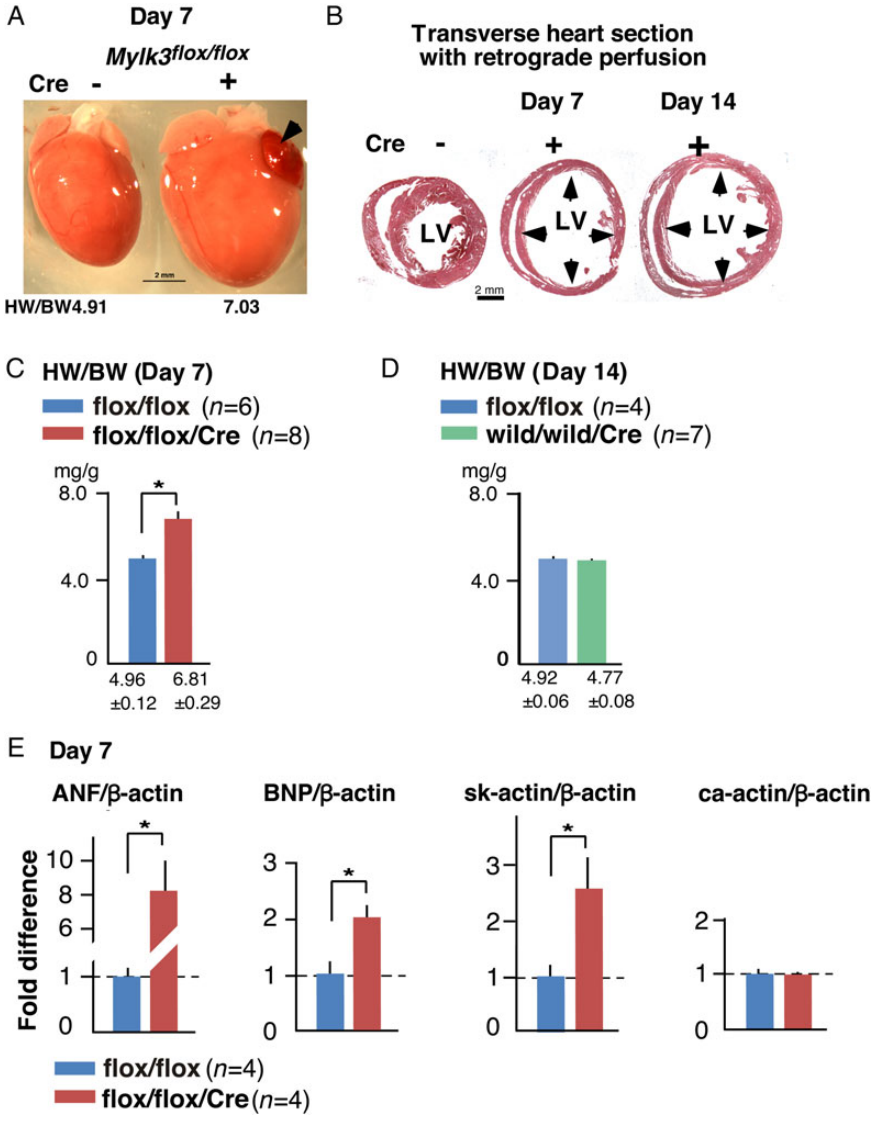

Figure 2 Acute heart failure in *Mylk3-KO* mice at Day 7 after tamoxifen injection. (*A*) Representative hearts with a HW/BW ratio. Arrowhead indicates congestion of left atrium. (*B*) Representative transverse sections of the heart arrested and fixed at diastole by retrograde perfusion belonging to control mice (Cre−) at Day 7 and *Mylk3-KO* mice (Cre+) at Days 7 and 14 after tamoxifen injection. (*C*) HW/BW ratio with mean BW of 19.9 ± 1.5 g ($Mylk3^{flox/flox}$, $n = 6$) vs. 19.7 ± 1.0 g ($Mylk3^{flox/flox}$/Cre, $n = 8$). (*D*) HW/BW ratio with mean BW of 19.2 ± 1.0 g ($Mylk3^{flox/flox}$, $n = 4$) vs. 20.9 ± 0.5 g ($Mylk3^{+/+}$/Cre, $n = 7$). (*E*) Real-time RT-PCR shows fold differences in mRNA of ANF, BNP, skeletal actin, and control cardiac actin relative to β-actin with the value of $Mylk3^{flox/flox}$ defined as 1 (mean ± SEM, $n = 4$ each). $^*P < 0.05$.

end-systole compared with that at end-diastole, and reduced cardiac torsion, seen as reduced twisting motion, were also observed in *Mylk3-KO* mice (*Figure 3A*).

Echocardiography was performed on Days 0, 7, and 14 after injection of tamoxifen in both *Mylk3-KO* mice and their two control groups (*Figure 3B* and see Supplementary material online, *Figure S1*). Consistent with the MRI studies, there were reductions in cardiac contractility and increases in the dimensions of the left ventricular cavity both on Days 7 and 14 after injections of tamoxifen in *Mylk3-KO* mice, but not in the two control groups. Further analyses showed that reduction of contractility started as early as Day 4 using serial echocardiography, corresponding to the reduction of cMLCK protein expression (*Figures 3C* and *1C*).

Haemodynamic measurements by left ventricular catheterization showed that *Mylk3-KO* mice exhibited reduced rates of contraction (+d*P*/d*t*) and relaxation (−d*P*/d*t*), increased left ventricular volume, and markedly reduced preload recruitable stroke work, which defines LV performance independently from the loading conditions (*Figure 3D*). Overall, detailed functional analyses on Day 7 after tamoxifen injection showed that *Mylk3-KO* mice were in acute heart failure with reduced contractility.

3.3 Cardiomyocyte atrophy, cell death, and impaired Ca^{2+} handling in *Mylk3-KO* mice

Histological analyses revealed severely convoluted, and wavy, cardiomyocytes, which had an abnormal sarcomeric structure, along with increased fibrosis in the hearts from *Mylk3-KO* mice when compared with their controls (*Figure 4A–C*). The number of TUNEL-positive nuclei

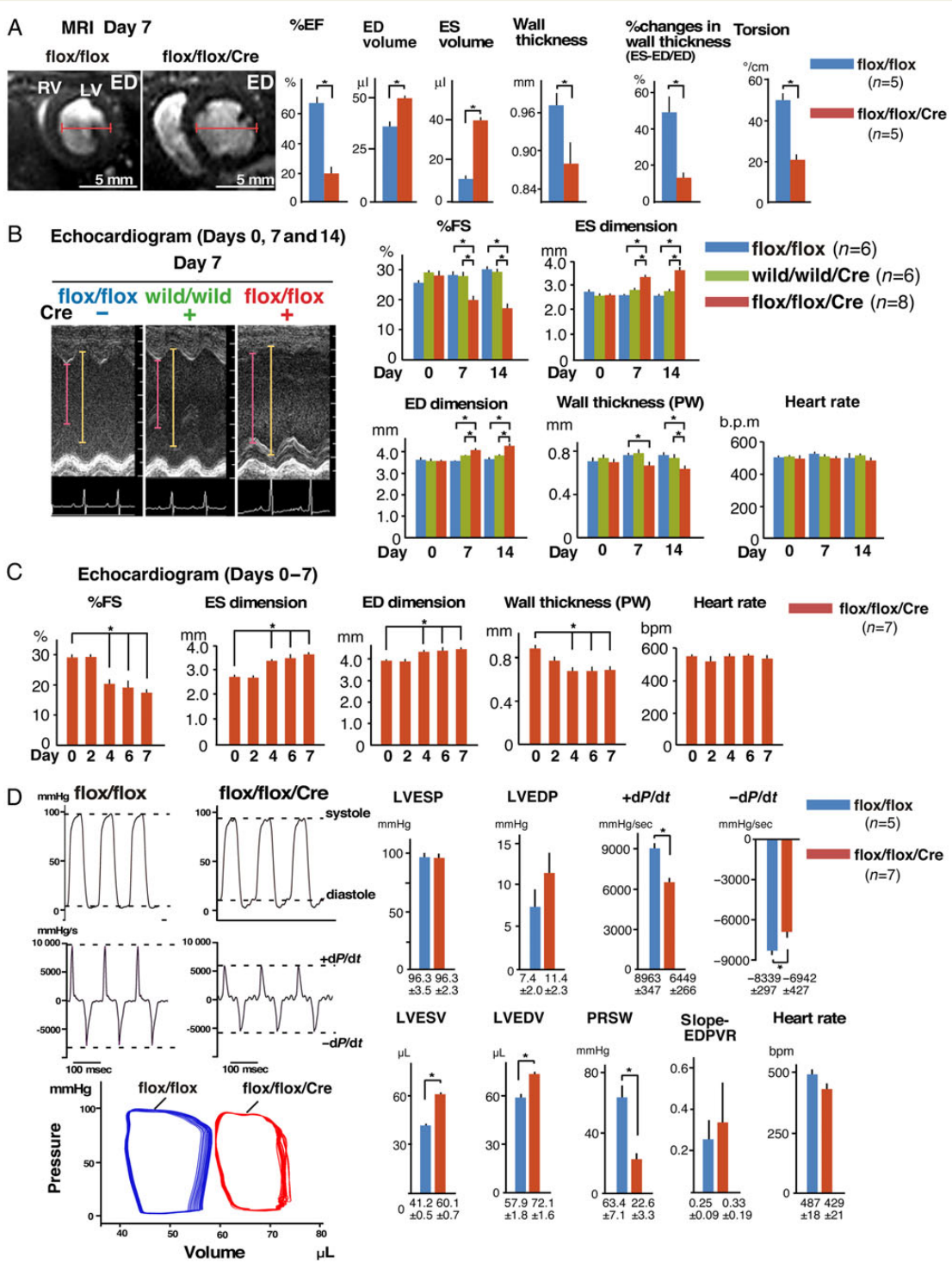

Figure 3 Reduced contractility of *Mylk3-KO* mice. (*A*) Representative MRI images, and analysed data for cardiac contraction, wall volume, wall thickness, and torsion, examined using MRI at Day 7 after tamoxifen injection. Bars = 5 mm. Cardiac contraction and torsion examined using MRI (mean ± SE, $n = 5$ each). (*B*) Echocardiographic indices of *Mylk3-KO* mice ($n = 8$) and two controls (*Mylk3*$^{flox/flox}$ and *Mylk3*$^{+/+}$/*αMHCmerCremer*, $n = 6$ each) before and at Days 7 and 14 after tamoxifen injection. Time-dependent effects were not significant for ED dimension or HR using repeated-measure ANOVA. (*C*) Echocardiographic indices of *Mylk3-KO* mice ($n = 7$) before, and Days 2, 4, and 6 after tamoxifen injection. Time-dependent effects were analysed by repeated-measure ANOVA. (*D*) Representative tracing of LV pressure, d*P*/d*t*, LVPV curve, and summarized data at Day 7 after tamoxifen injection from *Mylk3-KO* mice ($n = 7$) and control *Mylk3*$^{flox/flox}$ ($n = 5$). $^*P < 0.05$.

relative to the total nuclei is also increased in *Mylk3-KO* mice compared with the controls (*Figure 4D*), suggesting additional involvement of apoptosis for cell death.

When the heart was arrested and fixed at end-diastole by retrograde perfusion, the wavy cardiomyocytes were found to be more straight, elongated, and thinner than controls (*Figure 4E*). TEM from

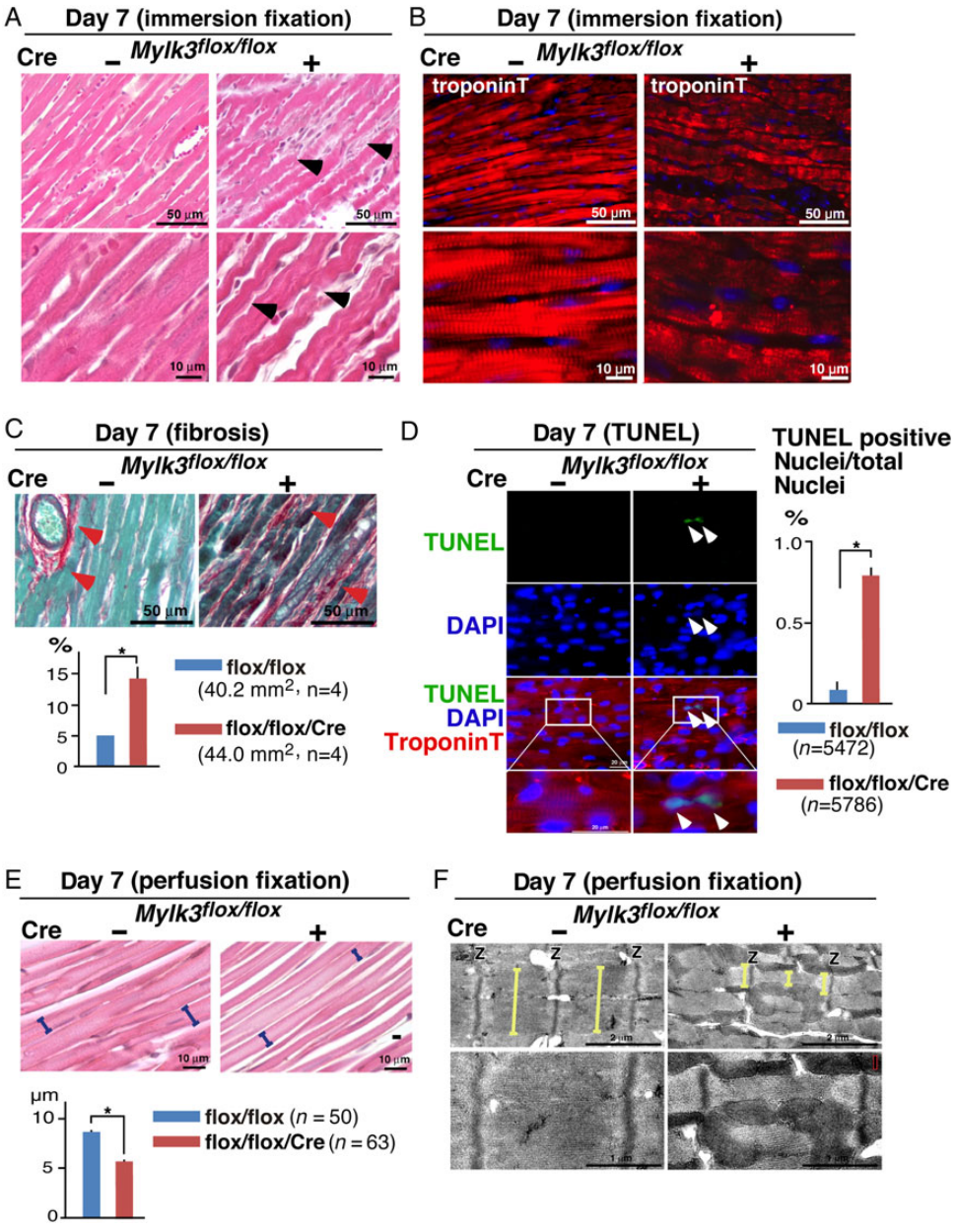

Figure 4 Cardiomyocyte atrophy and cell death of *Mylk3-KO* mice. (*A*) Representative H&E stained hearts with immersion fixation. Convoluted cardiomyocytes in *Mylk3-KO* are marked with arrowheads. (*B*) Representative immunofluorescent images of troponin T-stained hearts with immersion fixation. (*C*) Representative images of Picro Sirius red-stained hearts and area size of fibrosis (per cent relative to the total area examined, $n = 4$ each). (*D*) Representative TUNEL staining and the relative number of TUNEL-positive nuclei (per cent relative to the total nuclei examined, *Mylk3*$^{flox/flox}$, $n = 5472$; *Mylk3*$^{flox/flox}$/Cre, $n = 5786$ from $n = 3$ mice each). (*E*) Representative H&E stained hearts following retrograde perfusion fixation, and LV cell width examined at the nuclei level (*Mylk3*$^{flox/flox}$, $n = 50$ from three mice, *Mylk3*$^{flox/flox}$/Cre, $n = 63$ from four mice). (*F*) Representative TEM of the LV. Yellow bars represent the width of single sarcomere. *$P < 0.05$.

the hearts arrested and fixed at end-diastole revealed the anticipated alignment of adjacent sarcomeres in the control hearts, but not in the hearts from *Mylk3-KO* mice (*Figure 4F*). In the *Mylk3-KO* mice, sarcomeres were thinner, and the width of single sarcomeres varied within a single myocyte.

Consistently, cardiomyocytes isolated from *Mylk3-KO* mice were longer and thinner than their controls, showing an increased ratio between their long and short axes (*Figure 5A*). They also showed marked reductions in contractility and rates of contraction and relaxation (*Figure 5B*). A reduction of amplitude of the intracellular Ca^{2+} transient, increased diastolic fluorescent ratio, and Ca^{2+} decay speed suggested the presence of Ca^{2+}-handling abnormalities during diastole in inducible *Mylk3-KO* mice. On the other hand, as described in our previous study,[17] germline *Mylk3* knockout (*Mylk3*$^{-/-}$) hearts did not demonstrate the Ca^{2+}-handling abnormalities.

SERCA2a and its regulatory protein phospholamban[24,25] are predominantly responsible for Ca^{2+} restoration into the sarcoplasmic reticulum (SR) during diastole. Reduced mRNA expression of

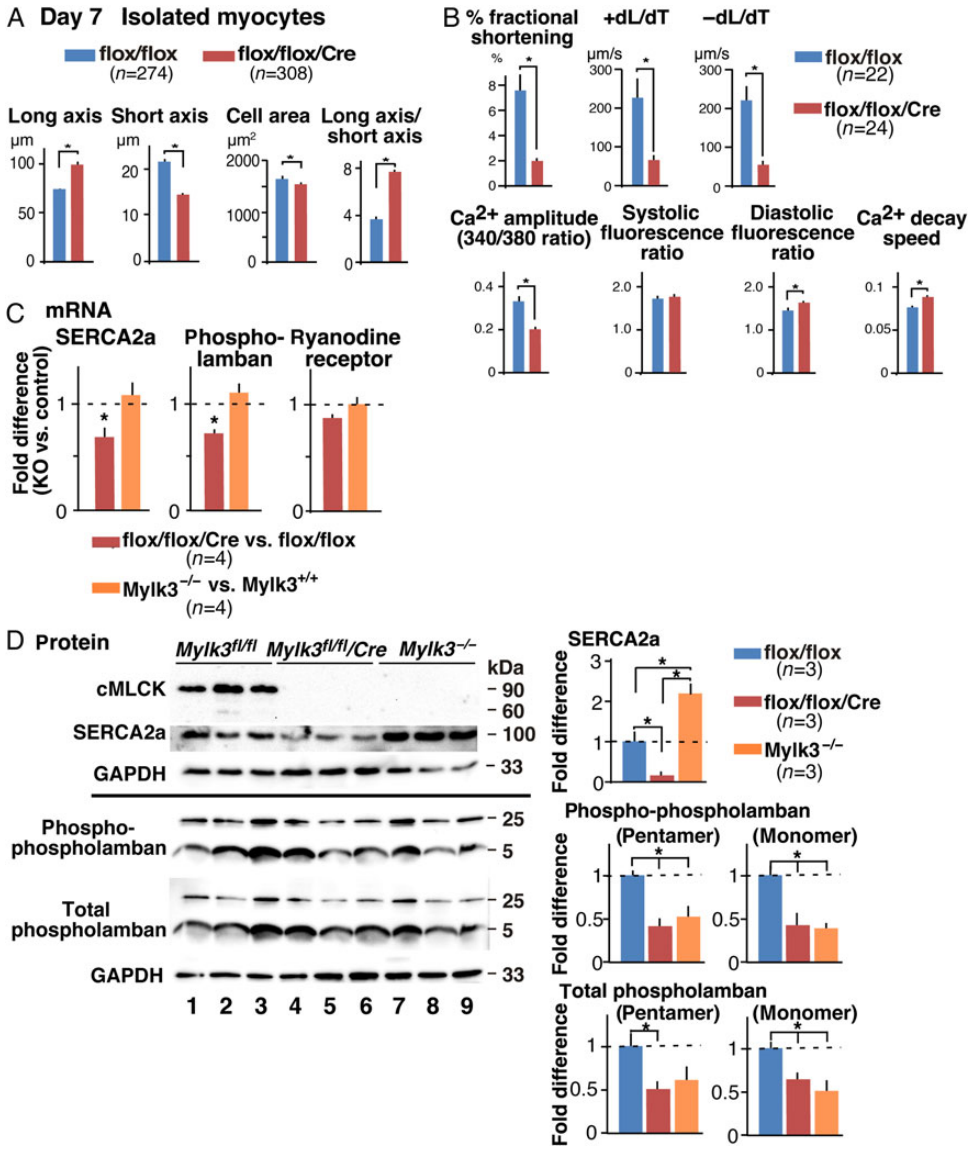

Figure 5 Longer and thinner cardiomyocytes with reduced contractility and impaired Ca^{2+}-handling in *Mylk3-KO* mice. (*A*) Summarized data of short and long axes, cell area size, and ratio of long vs. short axis of cardiomyocytes isolated at Day 7 after tamoxifen injection ($Mylk3^{flox/flox}$, $n = 274$; $Mylk3^{flox/flox}$/Cre, $n = 308$ from $n = 4$ mice each). (*B*) Measurements of cardiac contraction and simultaneous Ca^{2+} transients in isolated cardiomyocytes ($Mylk3^{flox/flox}$, $n = 22$; $Mylk3^{flox/flox}$/Cre, $n = 24$ from $n = 3$ mice each). (*C*) RT-PCR shows fold differences in mRNA of SERCA2a, phospholamban, and ryanodine receptor relative to β-actin in inducible and germline *Mylk3* knockout mice with the value of $Mylk3^{flox/flox}$ or $Mylk3^{+/+}$ defined as 1 (mean ± SEM, $n = 4$ each). (*D*) Western blotting shows SERCA2a as well as Ser^{16}-phosphorylated and total phospholamban expression in inducible and germline *Mylk3* knockout mice relative to GAPDH with the value in $Mylk3^{flox/flox}$ defined as 1 (mean ± SEM, $n = 3$ each). $^*P < 0.05$.

SERCA2a and phospholamban was uniquely demonstrated in inducible *Mylk3-KO*, but not in germline $Mylk3^{-/-}$ mice (*Figure 5C*). Western blotting confirmed the reduction of SERCA2a in inducible *Mylk3-KO* and oppositely a slight increase in $Mylk3^{-/-}$ mice (*Figure 5D*). Expression of SERCA2a's negative regulator, phospholamban, was reduced in inducible *Mylk3-KO* mice. The degree of its reduction, however, was less than that of SERCA2a, and was not specific in inducible *Mylk3-KO* mice, as seen in germline $Mylk3^{-/-}$ mice except for the total pentameric form of phospholamban (*Figure 5D*). Taken overall, inducible *Mylk3-KO* mice uniquely demonstrate Ca^{2+}-handling abnormalities, accompanied by reduction of SERCA2a expression compared with germline *Mylk3* knockout mice.

3.4 Marked reduction/absence of MLC2v phosphorylation without a compensatory increase of other kinases shown to phosphorylate MLC2 in inducible and germline *Mylk3* knockout mice

Despite skeletal and smooth muscle MLCK and Dapk3/ZIPK having been shown to phosphorylate MLC2,[8,26,27] MLC2 phosphorylation was markedly reduced or absent in inducible *Mylk3-KO* (Day 7 following tamoxifen injection) and germline $Mylk3^{-/-}$ mice[17] (*Figure 6A*). Consistent with that finding, there were no compensatory increases of mRNA of these kinases in either inducible or germline *Mylk3* knockout mice (*Figure 6B*).

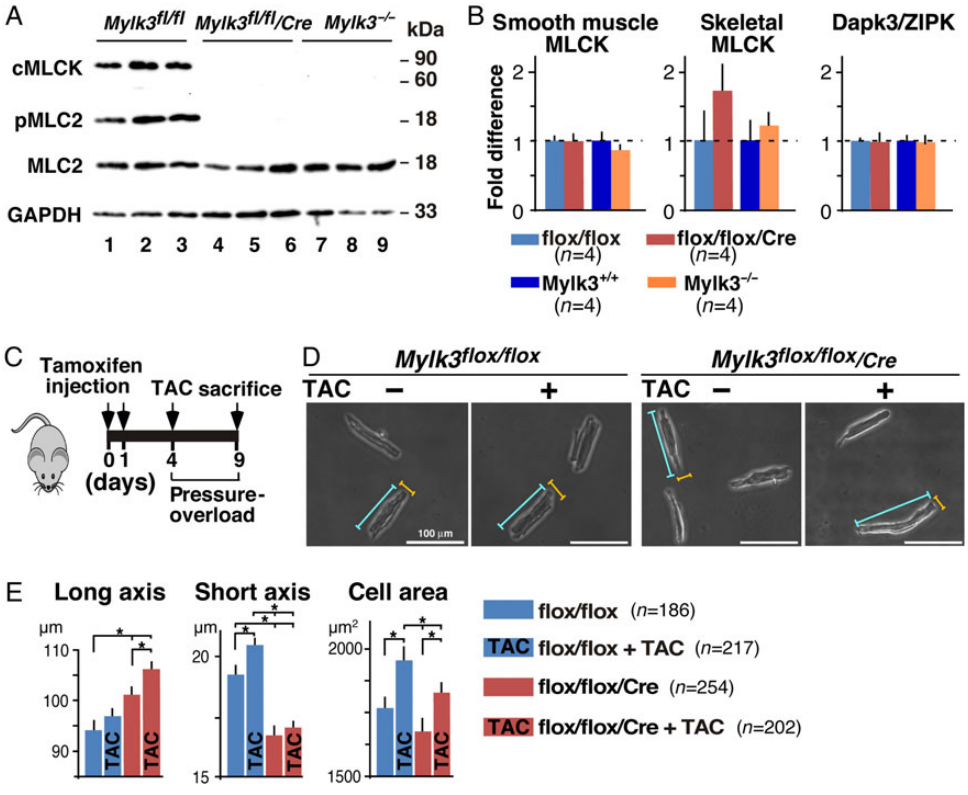

Figure 6 No compensatory increases of smooth muscle and skeletal MLCK, and Dapk3/ZIPK both in *Mylk3-KO* and *Mylk3*$^{-/-}$ mice and attenuation of adaptive thickening after pressure overload in *Mylk3-KO* mice. (*A*) Western blotting shows markedly reduced or absent cMLCK and phosphorylated MLC2v in inducible (day 7 following tamoxifen injection) and germline *Mylk3* knockout mice. (*B*) Real-time RT-PCR showing fold differences in mRNA of smooth muscle and skeletal MLCK, and Dapk3/ZIPK relative to β-actin in inducible (Day 7 following tamoxifen injection) and germline *Mylk3* knockout mice with the value in *Mylk3*$^{flox/flox}$ or *Mylk3*$^{+/+}$ defined as 1 (mean ± SEM, $n = 4$ each). (*C*) Time course experimental design for pressure overload and tamoxifen injections. (*D*) Representative images of cardiomyocytes with or without TAC after tamoxifen injection. Examples of short axis (yellow line) and long axis (blue line) are indicated. (*E*) Summarized data for the short and long axes, and cell area size. Number of cells examined: *Mylk3*$^{flox/flox}$, $n = 308$ from four mice; *Mylk3*$^{flox/flox}$ with TAC, $n = 217$ from three mice; *Mylk3-KO*, $n = 252$ from three mice; and *Mylk3-KO* with TAC, $n = 202$ from four mice. *$P < 0.05$.

3.5 Attenuation of pressure overload hypertrophy in *Mylk3-KO* mice

Finally, in order to examine whether reduction of cMLCK is involved in the transition from initial adaptive thickening of cardiomyocytes to a subsequent elongation,[3–6] we subjected the *Mylk3-KO* mice to transaortic constriction (TAC) on Day 4 when cMLCK expression was markedly reduced. We then examined for the presence of anticipated adaptive cardiomyocytic thickening on Day 9 (*Figure 6C*). Adaptive thickening, as revealed by an increase in short axis width and increased cell area, was observed in control mice after 5 days of sustained pressure overload. In contrast, the cardiomyocytes from *Mylk3-KO* mice were further elongated, showing no evidence of thickening (*Figure 6D* and *E*).

4. Discussion

Our major finding is that rapid, progressive, and profound heart failure, accompanied by sarcomeric atrophy, occurs shortly after elimination of cMLCK in adult mice. Pressure overload did not induce adaptive cardiomyocyte thickening in the absence of cMLCK. MLC2 phosphorylation, which has been shown to stabilize the actin–myosin interaction,[7–13] was markedly reduced or absent in inducible *Mylk3-KO* and germline *Mylk3*$^{-/-}$ mice corresponding to the absence of cMLCK. There was no significant induction of other potential MLC2v kinases, including skeletal and smooth muscle MLCK, and Dapk3/ZIPK3.[8,26,27] In human heart failure, MLC2v phosphorylation is known to be reduced from ~30 to 40% in healthy hearts to ~18% of total MLC2v.[28,29]

Severely convoluted cardiomyocytes with sarcomeric disorganization, wavy fibres, and cell death were demonstrated in *Mylk3-KO* mice, and prevented normal contractile forces, thus leading to heart failure. The pathological finding named 'attenuated wavy fibre' is sometimes observed in acute and chronic heart failure in humans and animal models.[30–34] It is extensively recognized in canine species as one of the criteria for dilated cardiomyopathy.[32,35] The underlying mechanism is not fully understood, and the waviness may be an artefact *in vitro*, reflecting the loss of volume distention. This partly agrees with findings in *Mylk3-KO* mice, in which waviness was not evident with light microscopy when the heart was arrested and fixed at the diastole. TEM analysis following perfusion fixation, however, did not show the anticipated alignment of sarcomeres in the hearts from *Mylk3-KO* mice, suggesting that attenuated wavy fibres might reflect additional specific disease processes.

Intracellular Ca^{2+} homeostasis is well balanced in normal hearts, but is altered in a number of human and rodent heart failure models, and is responsible for depressed contractility.[36–38] In *Mylk3-KO* mice, a reduction of SERCA2a proteins of almost three-quarters will result in reduced SR Ca^{2+} uptake and Ca^{2+} amplitude in cardiomyocytes, leading to impaired cardiomyocyte contractility. This is partly attributed to the reduction in SERCA2a mRNA by reduced transcription. Multiple factors have been shown to regulate SERCA2a transcription, including the nuclear factor of activated T cells (NFATs), thyroid hormone with thyroid hormone receptor complex, SP1, and P38.[39,40] Changes in intracellular Ca^{2+} load in *Mylk3-KO* mice might modulate the activity of Ca^{2+}-dependent kinases and phosphates, such as Ca^{2+}–calmodulin-dependent kinases and calcineurin–NFAT signalling pathways.[38,41] Effects of less profound reduction of both monomeric- and pentameric-phospholamban, which would lift the inhibition of SERCA2a functions,[24,25] on the reduction of SR Ca^{2+} uptake in inducible *Mylk3-KO* cardiomyocytes remain unclear. Of note, crosstalking among Ca^{2+}-handling proteins has been speculated, as phospholamban is also decreased in SERCA2a$^{+/-}$ mice.[42] Impaired Ca^{2+}-handling was unique to inducible *Mylk3-KO* and was not evident in germline *Mylk3*$^{-/-}$ mice under similar experimental conditions.[17] In addition, the sarcomeric disorganization, wavy fibres, and interstitial fibrosis shown in inducible *Mylk3-KO* hearts were absent in germline *Mylk3*$^{-/-}$ mice. Instead, these mice showed compensatory cardiomyocyte hypertrophy.[17] Similarly, in germline knock-in mice that express the non-phosphorylatable MLC2v mutant, Ser14/15Ala,[12] thinner cardiomyocytes are not found under sedentary conditions. Additional stressors, such as pressure overloading or swimming exercise, are required to make cardiomyocytes thinner rather than thicker.

Despite the fact that skeletal and smooth muscles MLCK and Dapk3/ZIPK have been shown to phosphorylate MLC2,[8,26,27] MLC2 phosphorylation was markedly reduced or absent in inducible *Mylk3-KO* and germline *Mylk3*$^{-/-}$ mice without compensatory increases of the mRNA of these kinases. The phenotypic difference between germline *Mylk3*$^{-/-}$ or MLC2v mutant mice and inducible *Mylk3-KO* mice could solely be due to the absence of rapid and inducible phosphorylation of MLC2, or due to the absence of cMLCK itself in adult mice. For instance, kinase-independent functions have been well established in cytoskeletal organization, cell migration, aggregation, and cell membrane tension in smooth muscle MLCK, primarily due to the F-actin binding of smooth muscle MLCK through a repeat motif (DFRXXL).[43–45] cMLCK, however, does not contain the putative F-actin binding DERXXL motif[15] and does not bind to cardiac actin (data not shown). These possibilities, which are beyond the scope of the current study, require additional future investigations.

To mitigate the possibility that a high dose of tamoxifen, such as 80 mg/kg/day given over 5 days (total 400 mg/kg), would result in heart failure,[23] we utilized a substantially lower dose, specifically 50 mg/kg/day given over 2 days. Furthermore, we included a second control, *Mylk3*$^{+/+}$*/merCremer* mice, which showed no change in the ratio between HW/BW, nor contractility, subsequent to injection of tamoxifen. Consistently, the total amount of tamoxifen we used in the current study, namely 100 mg/kg, is below the level known to produce cardiac toxicity and within the recommended doses as shown in multiple studies. These values were a total of 80–120 mg/kg, with 20 mg/kg/day given over 4–6 days as described in the original study which generated and characterized *αMHCmerCremer* mice,[18] and a total of 120 mg/kg, with 40 mg/kg/day given over 3 days.[46]

Pressure overload by TAC is widely used to evoke hypertrophy in animal models so as to understand the processes of cardiac remodelling. In the clinical setting, however, left ventricular pressure overload occurs more chronically, as seen in long-standing systemic hypertension or left ventricular outflow tract obstruction. The difference between the experimental and clinical settings represents one of the limitations of the experimental design of the current study. To understand the role of cMLCK in TAC-induced cardiac hypertrophy, pressure overload was initiated on Day 4 following tamoxifen injection, when expression of cMLCK protein begins to be markedly reduced. At the same time, cardiac contractility starts to decline rapidly. Thus, the interpretation of the data regarding the absence of TAC-induced cardiac hypertrophy in inducible *Mylk3-KO* mice also needs to take account of the complex secondary effects resulting from the heart failure itself.

In summary, we have created novel adult inducible *Mylk3-KO* mice, which suffer rapid and profound heart failure. In these mice, furthermore, pressure overload did not induce initial adaptive cardiomyocytic thickening. Our findings suggest that the mouse model is likely to provide important insights into the molecular mechanisms underlying the transition from adaptive hypertrophy to heart failure by pressure overload.

Supplementary material

Supplementary material is available at *Cardiovascular Research* online.

Acknowledgements

We greatly appreciate the help of D.W. Benson and H. Wakimoto for critical reading of the manuscript; and D. Smith, M. Hoshijima, E. Chan, Y. Ikeda, M. Zárate, and K. Fortin for their valuable suggestions and technical support. During preparation of the present manuscript, adult inducible *Mylk3-KO* mice were generated and reported independently.[47]

Conflict of interest: none declared.

Funding

This work was supported by American Heart Association (14GRNAT20380822 to H.K.); National Institute of Health (HL081577 to H.K., HL89200 to R.L.M.); and University of Florida (Medical Science Research Program to M.T.M.; College of Medicine Scholars Program to A.M.H.; and Opportunity Fund to H.K.)

References

1. Askoxylakis V, Thieke C, Pleger ST, Most P, Tanner J, Lindel K, Katus HA, Debus J, Bischof M. Long-term survival of cancer patients compared to heart failure and stroke: a systematic review. *BMC Cancer* 2010;**10**:105.
2. Jessup M, Brozena S. Heart failure. *N Engl J Med* 2003;**348**:2007–2018.
3. Diwan A, Dorn GW II. Decompensation of cardiac hypertrophy: cellular mechanisms and novel therapeutic targets. *Physiology (Bethesda)* 2007;**22**:56–64.
4. Balasubramanian S, Johnston RK, Moschella PC, Mani SK, Tuxworth WJ Jr, Kuppuswamy D. mTOR in growth and protection of hypertrophying myocardium. *Cardiovasc Hematol Agents Med Chem* 2009;**7**:52–63.
5. Russell B, Curtis MW, Koshman YE, Samarel AM. Mechanical stress-induced sarcomere assembly for cardiac muscle growth in length and width. *J Mol Cell Cardiol* 2010;**48**:817–823.
6. Rosca MG, Tandler B, Hoppel CL. Mitochondria in cardiac hypertrophy and heart failure. *J Mol Cell Cardiol* 2013;**55**:31–41.
7. Sanbe A, Fewell JG, Gulick J, Osinska H, Lorenz J, Hall DG, Murray LA, Kimball TR, Witt SA, Robbins J. Abnormal cardiac structure and function in mice expressing nonphosphorylatable cardiac regulatory myosin light chain 2. *J Biol Chem* 1999;**274**:21085–21094.

8. Davis JS, Hassanzadeh S, Winitsky S, Lin H, Satorius C, Vemuri R, Aletras AH, Wen H, Epstein ND. The overall pattern of cardiac contraction depends on a spatial gradient of myosin regulatory light chain phosphorylation. *Cell* 2001;**107**:631–641.
9. Moss RL, Fitzsimons DP. Myosin light chain 2 into the mainstream of cardiac development and contractility. *Circ Res* 2006;**99**:225–227.
10. Stelzer JE, Patel JR, Moss RL. Acceleration of stretch activation in murine myocardium due to phosphorylation of myosin regulatory light chain. *J Gen Physiol* 2006;**128**: 261–272.
11. Scruggs SB, Solaro RJ. The significance of regulatory light chain phosphorylation in cardiac physiology. *Arch Biochem Biophys* 2011;**510**:129–134.
12. Sheikh F, Ouyang K, Campbell SG, Lyon RC, Chuang J, Fitzsimons D, Tangney J, Hidalgo CG, Chung CS, Cheng H, Dalton ND, Gu Y, Kasahara H, Ghassemian M, Omens JH, Peterson KL, Granzier HL, Moss RL, McCulloch AD, Chen J. Mouse and computational models link Mlc2v dephosphorylation to altered myosin kinetics in early cardiac disease. *J Clin Invest* 2012;**122**:1209–1221.
13. Sheikh F, Lyon RC, Chen J. Getting the skinny on thick filament regulation in cardiac muscle biology and disease. *Trends Cardiovasc Med* 2013;**24**:133–141.
14. Seguchi O, Takashima S, Yamazaki S, Asakura M, Asano Y, Shintani Y, Wakeno M, Minamino T, Kondo H, Furukawa H, Nakamaru K, Naito A, Takahashi T, Ohtsuka T, Kawakami K, Isomura T, Kitamura S, Tomoike H, Mochizuki N, Kitakaze M. A cardiac myosin light chain kinase regulates sarcomere assembly in the vertebrate heart. *J Clin Invest* 2007;**117**:2812–2824.
15. Chan JY, Takeda M, Briggs LE, Graham ML, Lu JT, Horikoshi N, Weinberg EO, Aoki H, Sato N, Chien KR, Kasahara H. Identification of cardiac-specific myosin light chain kinase. *Circ Res* 2008;**102**:571–580.
16. Ding P, Huang J, Battiprolu PK, Hill JA, Kamm KE, Stull JT. Cardiac myosin light chain kinase is necessary for myosin regulatory light chain phosphorylation and cardiac performance in vivo. *J Biol Chem* 2010;**285**:40819–40829.
17. Warren SA, Briggs LE, Zeng H, Chuang J, Chang EI, Terada R, Li M, Swanson MS, Lecker SH, Willis MS, Spinale FG, Maupin-Furlowe J, McMullen JR, Moss RL, Kasahara H. Myosin light chain phosphorylation is critical for adaptation to cardiac stress. *Circulation* 2012;**126**:2575–2588.
18. Sohal DS, Nghiem M, Crackower MA, Witt SA, Kimball TR, Tymitz KM, Penninger JM, Molkentin JD. Temporally regulated and tissue-specific gene manipulations in the adult and embryonic heart using a tamoxifen-inducible Cre protein. *Circ Res* 2001;**89**:20–25.
19. Warren SA, Terada R, Briggs LE, Cole-Jeffrey CT, Chien WM, Seki T, Weinberg EO, Yang TP, Chin MT, Bungert J, Kasahara H. Differential role of Nkx2–5 in activation of the atrial natriuretic factor gene in the developing versus failing heart. *Mol Cell Biol* 2011;**31**:4633–4645.
20. Pacher P, Nagayama T, Mukhopadhyay P, Batkai S, Kass DA. Measurement of cardiac function using pressure-volume conductance catheter technique in mice and rats. *Nat Protoc* 2008;**3**:1422–1434.
21. Takeda M, Briggs LE, Wakimoto H, Marks MH, Warren SA, Lu JT, Weinberg EO, Robertson KD, Chien KR, Kasahara H. Slow progressive conduction and contraction defects in loss of Nkx2–5 mice after cardiomyocyte terminal differentiation. *Lab Invest* 2009;**89**:983–993.
22. Conti E, Izaurralde E. Nonsense-mediated mRNA decay: molecular insights and mechanistic variations across species. *Curr Opin Cell Biol* 2005;**17**:316–325.
23. Koitabashi N, Bedja D, Zaiman AL, Pinto YM, Zhang M, Gabrielson KL, Takimoto E, Kass DA. Avoidance of transient cardiomyopathy in cardiomyocyte-targeted tamoxifen-induced MerCreMer gene deletion models. *Circ Res* 2009;**105**:12–15.
24. Ather S, Respress JL, Li N, Wehrens XH. Alterations in ryanodine receptors and related proteins in heart failure. *Biochim Biophys Acta* 2013;**1832**:2425–2431.
25. Wittmann T, Lohse MJ, Schmitt JP. Phospholamban pentamers attenuate PKA-dependent phosphorylation of monomers. *J Mol Cell Cardiol* 2015;**80**:90–97.
26. Herring BP, Dixon S, Gallagher PJ. Smooth muscle myosin light chain kinase expression in cardiac and skeletal muscle. *Am J Physiol Cell Physiol* 2000;**279**:C1656–C1664.
27. Chang AN, Chen G, Gerard RD, Kamm KE, Stull JT. Cardiac myosin is a substrate for zipper-interacting protein kinase (ZIPK). *J Biol Chem* 2010;**285**:5122–5126.
28. Morano I. Tuning the human heart molecular motors by myosin light chains. *J Mol Med* 1999;**77**:544–555.
29. van der Velden J, Papp Z, Boontje NM, Zaremba R, de Jong JW, Janssen PM, Hasenfuss G, Stienen GJ. The effect of myosin light chain 2 dephosphorylation on Ca^{2+}-sensitivity of force is enhanced in failing human hearts. *Cardiovasc Res* 2003;**57**: 505–514.
30. Eichbaum FW. 'Wavy' myocardial fibers in spontaneous and experimental adrenergic cardiopathies. *Cardiology* 1975;**60**:358–365.
31. Davies MJ. The cardiomyopathies: a review of terminology, pathology and pathogenesis. *Histopathology* 1984;**8**:363–393.
32. Tidholm A, Jonsson L. Histologic characterization of canine dilated cardiomyopathy. *Vet Pathol* 2005;**42**:1–8.
33. Chiu YT, Cheng CC, Lin NN, Hung YW, Chen YT, Hsu SL, Chi CS, Fu YC. High-dose norepinephrine induces disruption of myocardial extracellular matrix and left ventricular dilatation and dysfunction in a novel feline model. *J Chin Med Assoc* 2006;**69**: 343–350.
34. Kakimoto Y, Ito S, Abiru H, Kotani H, Ozeki M, Tamaki K, Tsuruyama T. Sorbin and SH3 domain-containing protein 2 is released from infarcted heart in the very early phase: proteomic analysis of cardiac tissues from patients. *J Am Heart Assoc* 2013;**2**:e000565.
35. Lobo L, Carvalheira J, Canada N, Bussadori C, Gomes JL, Faustino AM. Histologic characterization of dilated cardiomyopathy in Estrela mountain dogs. *Vet Pathol* 2010;**47**: 637–642.
36. Houser SR, Piacentino V III, Weisser J. Abnormalities of calcium cycling in the hypertrophied and failing heart. *J Mol Cell Cardiol* 2000;**32**:1595–1607.
37. Bers DM. Cardiac excitation-contraction coupling. *Nature* 2002;**415**:198–205.
38. Mattiazzi A, Bassani RA, Escobar AL, Palomeque J, Valverde CA, Vila Petroff M, Bers DM. Chasing cardiac physiology and pathology down the CaMKII cascade. *Am J Physiol Heart Circ Physiol* 2015;**308**:H1177–H1191.
39. Vlasblom R, Muller A, Musters RJ, Zuidwijk MJ, Van Hardeveld C, Paulus WJ, Simonides WS. Contractile arrest reveals calcium-dependent stimulation of SERCA2a mRNA expression in cultured ventricular cardiomyocytes. *Cardiovasc Res* 2004;**63**: 537–544.
40. Zarain-Herzberg A, Estrada-Aviles R, Fragoso-Medina J. Regulation of sarco(endo) plasmic reticulum Ca^{2+}-ATPase and calsequestrin gene expression in the heart. *Can J Physiol Pharmacol* 2012;**90**:1017–1028.
41. Heineke J, Ritter O. Cardiomyocyte calcineurin signaling in subcellular domains: from the sarcolemma to the nucleus and beyond. *J Mol Cell Cardiol* 2012;**52**:62–73.
42. Periasamy M, Huke S. SERCA pump level is a critical determinant of Ca(2+) homeostasis and cardiac contractility. *J Mol Cell Cardiol* 2001;**33**:1053–1063.
43. Soderling TR, Stull JT. Structure and regulation of calcium/calmodulin-dependent protein kinases. *Chem Rev* 2001;**101**:2341–2352.
44. Poperechnaya A, Varlamova O, Lin PJ, Stull JT, Bresnick AR. Localization and activity of myosin light chain kinase isoforms during the cell cycle. *J Cell Biol* 2000;**151**:697–708.
45. Chen C, Tao T, Wen C, He WQ, Qiao YN, Gao YQ, Chen X, Wang P, Chen CP, Zhao W, Chen HQ, Ye AP, Peng YJ, Zhu MS. Myosin light chain kinase (MLCK) regulates cell migration in a myosin regulatory light chain phosphorylation-independent mechanism. *J Biol Chem* 2014;**101**:2341–2352.
46. Hall ME, Smith G, Hall JE, Stec DE. Systolic dysfunction in cardiac-specific ligand-inducible MerCreMer transgenic mice. *Am J Physiol Heart Circ Physiol* 2011;**301**: H253–H260.
47. Chang AN, Battiprolu PK, Cowley PM, Chen G, Gerard RD, Pinto JR, Hill JA, Baker AJ, Kamm KE, Stull JT. Constitutive phosphorylation of cardiac myosin regulatory light chain in vivo. *J Biol Chem* 2015;**290**:10703–10716.